

# Direct photons measured by the PHENIX experiment at RHIC

S. Bathe<sup>a</sup> for the PHENIX Collaboration

University of California, 900 University Avenue, Riverside, CA 92521, USA

Received: 22 August 2006 /

Published online: 9 December 2006 – © Springer-Verlag / Società Italiana di Fisica 2006

**Abstract.** Results from the PHENIX experiment at RHIC on direct photon production in  $p+p$ ,  $d+Au$ , and  $Au+Au$  collisions at  $\sqrt{s_{NN}} = 200$  GeV are presented. In  $p+p$  collisions, direct photon production at high  $p_T$  behaves as expected from perturbative QCD calculations. The  $p+p$  measurement serves as a baseline for direct photon production in  $Au+Au$  collisions. In  $d+Au$  collisions, no effects of cold nuclear matter are found within the large uncertainty of the measurement. In  $Au+Au$  collisions, the production of high  $p_T$  direct photons scales as expected for particle production in hard scatterings. This supports jet quenching models, which attribute the suppression of high  $p_T$  hadrons to the energy loss of fast partons in the medium produced in the collision. Low  $p_T$  direct photons, measured via  $e^+e^-$  pairs with small invariant mass, are possibly related to the production of thermal direct photons.

## 1 Introduction

Depending on their transverse momentum, direct photons convey information about different aspects of ultra-relativistic nucleus–nucleus ( $A+A$ ) collisions. High transverse momentum ( $p_T$ ) direct photons are produced in early, hard parton–parton scatterings by processes like quark–gluon Compton scattering ( $q+g \rightarrow q+\gamma$ ). Unlike scattered quarks or gluons, direct photons do not interact strongly with the medium subsequently produced in the collision. High  $p_T$  direct photons ( $p_T \gtrsim 6$  GeV/ $c$ ) therefore provide a baseline for measuring medium modifications of high  $p_T$  hadron production.

A significant fraction of low  $p_T$  direct photons ( $1 \leq p_T \leq 3$  GeV/ $c$  in central  $Au+Au$  collisions at  $\sqrt{s_{NN}} = 200$  GeV) is expected to come from a thermalized medium of deconfined quarks and gluons, the quark–gluon plasma (QGP), possibly created in  $A+A$  collisions [1]. These thermal photons carry information about the initial temperature of the QGP. Thermal photons are produced in the QGP as well as in the hadronic gas over the entire life time of the collision. The initial temperature can be extracted comparing measurements to models which convolute the production rate with the space-time evolution of the collision.

At low and intermediate  $p_T$  ( $p_T \leq 6$  GeV/ $c$  in central  $Au+Au$  collisions at  $\sqrt{s_{NN}} = 200$  GeV) another significant source of direct photons might be the interaction of fast partons from jets with thermal partons in the QGP [2] like  $q_{\text{hard}} + g_{\text{QGP}} \rightarrow q + \gamma$ .

Possible modifications of direct photon production from cold nuclear matter effects can be measured in  $d+Au$  collisions where no medium is created. Direct photon measurements in  $p+p$  collisions are a superb test of QCD. They constrain the gluon distribution function since the gluon is a direct participant of the partonic scattering. Furthermore, they provide a baseline for understanding direct photon production in  $A+A$  collisions.

## 2 High $p_T$ direct photons

### 2.1 Measurement

Experimentally, the measurement of direct photons is challenging due to a large background from hadron decays like  $\pi^0 \rightarrow \gamma\gamma$  and  $\eta \rightarrow \gamma\gamma$ . PHENIX measures all those photon sources. Photons are measured with the electromagnetic calorimeter (EMCal). Neutral pions and  $\eta$  mesons are measured through their two-photon decay branch [3, 4]. The EMCal [5] consists of six sectors of a lead scintillator and two sectors of a lead glass calorimeter centered at midrapidity ( $\eta < 0.35$ ) and covering 1/4 of the azimuthal angle.

The direct photon spectrum is obtained by subtracting the decay photon spectrum from the inclusive photon spectrum. This is gained from photon-like showers in the EMCal corrected for contaminations from charged hadrons and neutrons. The decay photon spectrum is calculated from the measured  $\pi^0$  and  $\eta$  spectrum, taking into account minor contributions from other hadrons that decay into photons.

If the detector occupancy is low as in  $p+p$  or  $d+Au$  collisions, the signal-to-background ratio can be improved

<sup>a</sup> e-mail: bathe@bnl.gov

Present Address: Brookhaven National Lab, Bldg. 510 C, Upton, NY 11973, USA

by event by event tagging of photons that have a matching partner as decay photons.

## 2.2 Results

### 2.2.1 $p + p$ collisions

The preliminary direct photon cross section for  $p + p$  collisions at  $\sqrt{s} = 200$  GeV is shown in Fig. 1 [6]. It is based on an integrated luminosity of  $266 \text{ nb}^{-1}$  collected in RHIC Run-3. For the whole  $p_T$  range of 5 to 16 GeV/c the observed cross section is consistent with a next-to-leading-order perturbative-QCD (NLO pQCD) calculation [7]. This measurement establishes a reference for direct photon production in  $A + A$ . In RHIC Run-5, PHENIX took a  $p + p$  data set with ten times the Run-3 statistics.

### 2.2.2 Au + Au collisions

The high  $p_T$  direct photon yield in  $A + A$  collisions relative to  $p + p$  is expected to scale with the parton luminosity in the overlap region of the two nuclei. The parton luminosity is quantified by the nuclear overlap function,  $T_{AA}$ . In the absence of nuclear effects the nuclear modification factor

$$R_{AA}(p_T) = \frac{dN/dp_T|_{A+A}}{\langle T_{AA} \rangle_f d\sigma/dp_T|_{p+p}} \quad (1)$$

is unity for particle production from hard scattering.

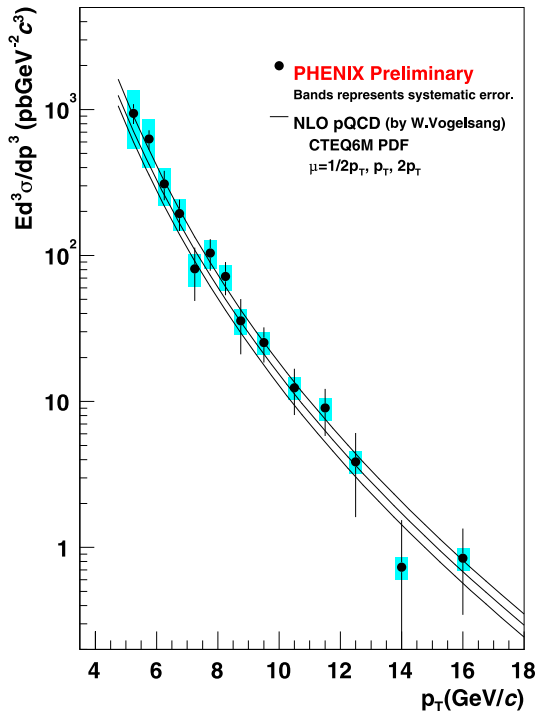


**Fig. 1.** Preliminary direct photon cross section as a function of  $p_T$  for  $p + p$  collisions at  $\sqrt{s} = 200$  GeV [6]. The solid curves are pQCD predictions [7] for three different scales, which represent the uncertainty on the calculation

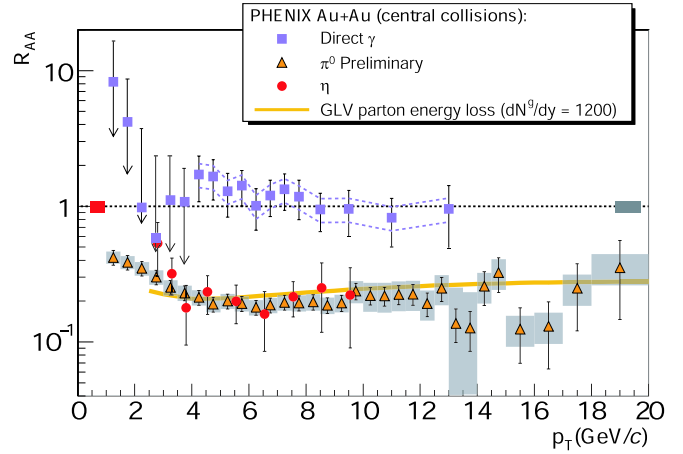


**Fig. 2.** Nuclear modification factor for direct photon,  $\pi^0$ , and  $\eta$  production in central Au + Au collisions at  $\sqrt{s_{NN}} = 200$  GeV. For direct photons, a pQCD calculation is used as the reference

As shown by PHENIX in RHIC Run-2 [8], at high  $p_T$  direct photon production is consistent with the  $T_{AA}$ -scaled pQCD expectation also in Au + Au collisions. Figure 2 compares the nuclear modification factor for direct photon,  $\pi^0$ , and  $\eta$  production in central Au + Au collisions at  $\sqrt{s_{NN}} = 200$  GeV. For direct photons, the pQCD calculation is used as a reference. The suppression for  $\pi^0$  and  $\eta$ , supported by the non-suppression of photons, can be described with energy loss of partons in the produced medium.

While high  $p_T$  direct photon production is consistent with the pQCD expectation, one should keep in mind that there are a number of medium effects that might alter direct photon production. On the one hand, a significant fraction of direct photons is expected to stem from the fragmentation of hard-scattered partons into jets. As those partons lose energy in the medium, also the fragmentation photons should be suppressed. On the other hand, as partons lose energy through gluon bremsstrahlung, they should also generate photon bremsstrahlung, enhancing the direct photon yield. It would be a coincidence if these counterbalancing effects exactly canceled.

Experimentally, contributions from these effects can be quantified by studying the azimuthal distribution of direct photon production with respect to the reaction plane. If fragmentation photons are suppressed, less direct photons are expected to be emitted outside of the reaction plane. If bremsstrahlung is enhanced, more direct photons will be found outside of the reaction plane.

### 2.2.3 $d + \text{Au}$ collisions

The preliminary direct photon yield for minimum-bias  $d + \text{Au}$  collisions at  $\sqrt{s_{NN}} = 200$  GeV is shown in the upper panel of Fig. 3 along with the yield in  $p + p$  collisions. The  $d + \text{Au}$  analysis is based on  $\approx 3$  billion events sampled in RHIC Run-3. The lower panel shows the ratio to the

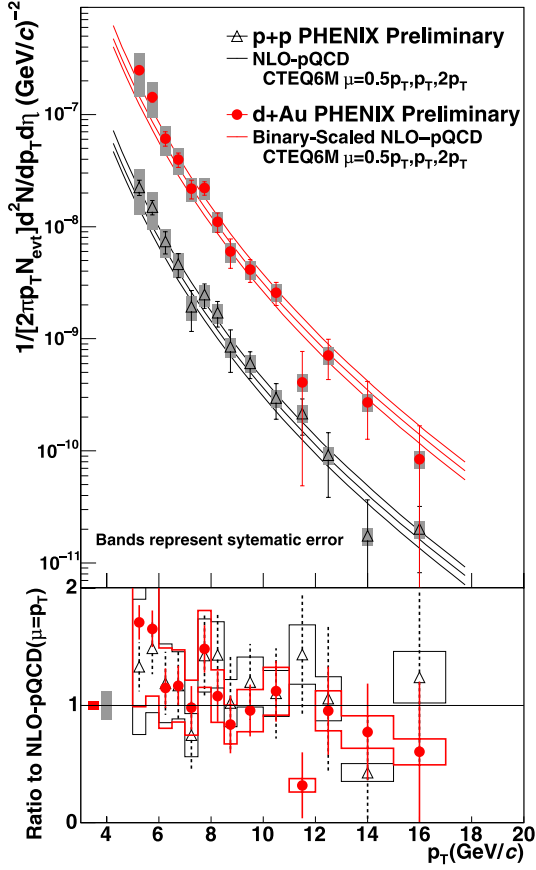


**Fig. 3.** Preliminary direct photon invariant yield as a function of  $p_T$  for  $p+p$  [6] and minimum-bias  $d+Au$  collisions at  $\sqrt{s_{NN}} = 200$  GeV. The *solid curves* are pQCD predictions [7] for three different scales, which represent the uncertainty on the calculation

$T_{AA}$ -scaled NLO pQCD calculation. The ratio is consistent with unity over the entire  $p_T$  range, showing no indication of cold nuclear matter effects. However, the uncertainty of the measurement is large. A high statistics  $d+Au$  run is planned.

### 3 Low $p_T$ direct photons

#### 3.1 Measurement

The EMCal measurement at low  $p_T$  suffers from a large background from decay photons. Also, the relative energy resolution of the EMCal becomes worse at low energy. Therefore, a new method [9, 10] to measure direct photons at low  $p_T$  has been employed. It has been carried out in heavy ion experiments for the first time. The method is based on the measurement of pairs of  $e^+e^-$ , which are identified with the PHENIX Ring Imaging Cherenkov Detector (RICH). The basic idea is that any source of real photons also produces virtual photons that decay into  $e^+e^-$  with small invariant mass. An example is the  $\pi^0$  Dalitz decay ( $\pi^0 \rightarrow \gamma e^+e^-$ ). This internal conversion method is

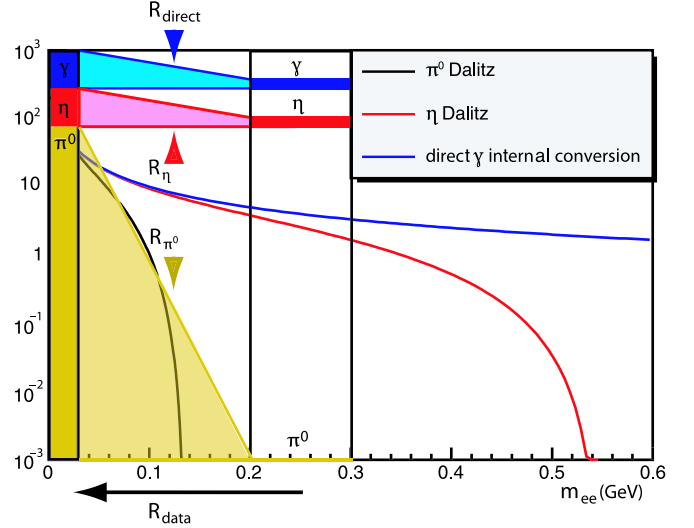


**Fig. 4.** Invariant-mass distribution of virtual photons from the  $\pi^0$  and  $\eta$  Dalitz decay as well as from direct photons according to (2). It is illustrated how the various contributions decrease to a fraction  $R$  when going to higher invariant mass with the  $\pi^0$  contribution exhausting

based on two assumptions: first, the ratio of direct-to-all photons is the same for real and virtual photons at small invariant mass close to zero ( $m_\gamma < 30$  MeV):  $\gamma_{\text{direct}}^*/\gamma_{\text{incl}}^* = \gamma_{\text{direct}}/\gamma_{\text{incl}}$ . Second, the mass distribution can be described by the Kroll–Wada formula [11], which has been established to describe the Dalitz decay<sup>1</sup>:

$$\frac{1}{N_\gamma} \frac{dN_{ee}}{dm_{ee}} = \frac{2\alpha}{3\pi} \sqrt{1 - \frac{4m_e^2}{m_{ee}^2}} \left(1 + \frac{2m_e^2}{m_{ee}^2}\right) \times \frac{1}{m_{ee}} |F(m_{ee}^2)|^2 \left(1 - \frac{m_{ee}^2}{M^2}\right)^3, \quad (2)$$

The mass distribution according to (2) is depicted in Fig. 4. For  $e^+e^-$  pairs from  $\pi^0$  and  $\eta$  Dalitz decays the yield is suppressed towards higher  $m_{ee}$  due to the mass,  $M$ , of the parent meson in the phase space factor  $(1 - m_{ee}^2/M^2)^3$  whereas no suppression takes place for  $e^+e^-$  pairs from virtual direct photons as long as  $m_{ee} \ll p_T^e$ . For the small invariant masses considered here the form factor  $|F(m_{ee}^2)|$  is assumed to be unity in all cases.

The key advantage of this method is the greatly improved signal-to-background ratio, which is achieved by eliminating the contribution from  $\pi^0$  Dalitz decays when the invariant mass is increased. In addition, the electron measurement through charged particle tracking provides a better energy resolution at low  $p_T$  than the EMCal photon measurement. This excellent energy resolution at low  $p_T$  combined with little material upstream of the detector,

<sup>1</sup> Since the virtual photons decay in the medium, this relation might be slightly modified. This would not affect the significance of the observed excess of direct photons, only its translation into an absolute yield of real direct photons.

where photons could convert generating background  $e^+e^-$  pairs, makes this measurement feasible in PHENIX.

The experimentally observed quantity is the ratio of  $e^+e^-$  pairs in an invariant mass bin where the  $\pi^0$  Dalitz decay is largely suppressed to the yield at an invariant mass close to zero:  $R_{\text{data}} = N_{ee}^{90-300 \text{ MeV}} / N_{ee}^{<30 \text{ MeV}}$ . If there is no direct photon signal,  $R_{\text{data}} = R_{\text{hadron}}^{\text{calc}}$ , *i.e.*  $R_{\text{data}}$  can be calculated<sup>2</sup> from (2) based on the known ratio  $\eta/\pi^0 = 0.45 \pm 0.1$ . An excess  $R_{\text{data}} > R_{\text{hadron}}^{\text{calc}}$  translates into the fraction of virtual direct photons at close to zero invariant mass according to:

$$\frac{\gamma_{\text{direct}}^*}{\gamma_{\text{incl}}^*} = \frac{R_{\text{data}} - R_{\text{hadron}}^{\text{calc}}}{R_{\text{direct } \gamma}^{\text{calc}} - R_{\text{hadron}}^{\text{calc}}}. \quad (3)$$

This can be derived starting from

$$R_{\text{data}} = N_{ee}^{90-300 \text{ MeV}} / N_{ee}^{<30 \text{ MeV}} \quad (4)$$

with

$$N_{ee} = N_{\text{hadron}} + N_{\text{direct } \gamma} \quad (5)$$

$$R_{\text{data}} = \frac{R_{\text{hadron}}^{\text{calc}} N_{\text{hadron}}^{<30 \text{ MeV}} + R_{\text{direct } \gamma}^{\text{calc}} N_{\text{direct } \gamma}^{<30 \text{ MeV}}}{N_{\text{hadron}}^{<30 \text{ MeV}} + N_{\text{direct } \gamma}^{<30 \text{ MeV}}} \quad (6)$$

$$= R_{\text{hadron}}^{\text{calc}} + (R_{\text{direct } \gamma}^{\text{calc}} - R_{\text{hadron}}^{\text{calc}}) \frac{N_{\text{direct } \gamma}^{<30 \text{ MeV}}}{N_{ee}^{<30 \text{ MeV}}}. \quad (7)$$

The direct photon spectrum is then obtained by multiplying  $\gamma_{\text{direct}}^*/\gamma_{\text{incl}}^*$  by the inclusive photon spectrum measured with the EMCal.

The full 2004 data set of about 900 million minimum bias events is analyzed. Events and centrality are selected as described in [12]. Electrons in the central arms are identified by matching charged particle tracks to clusters in the EMCal and to rings in the RICH detector. To obtain a clean invariant-mass distribution of  $e^+e^-$  pairs, pairs originating from photon conversions in the beam pipe or detector material are rejected based on their orientation with respect to the magnetic field. The combinatorial background is removed by an event-mixing technique. The uncertainty of the  $\eta$ -to- $\pi^0$  ratio of about 20% [13] is the main source of uncertainty, translating into an uncertainty of 20% of the measured direct photon yield. Other sources are the EMCal-measured inclusive photon yield (10%) and the  $e^+e^-$ -pair acceptance (5%). The total systematic uncertainty is 25%.

## 3.2 Results

Figure 5a shows the direct photon signal for central Au + Au collisions at  $\sqrt{s_{NN}} = 200 \text{ GeV}$  in terms of the double ratio  $(\gamma/\pi^0|_{\text{meas.}})/(\gamma/\pi^0|_{\text{bckgrd.}})$ . This ratio indicates a direct photon excess above the decay photon contribution as an enhancement above 1. In this figure,

<sup>2</sup> Besides  $\pi^0$  and  $\eta$ , decay photons from a cocktail of hadrons are considered here.

two measurements are compared: the result from the internal conversion method as described above [14] and a preliminary analysis of the conventional EMCal measurement based on a subset of the RHIC Run-4 data set [14].<sup>3</sup> While the internal conversion measurement results in a significant direct photon signal of about 10% above the decay photon background for  $1 < p_T < 5 \text{ GeV}/c$ , the EMCal measurement does not yield a significant direct photon signal below  $p_T = 3 \text{ GeV}/c$ , but agrees with the internal conversion measurement within the uncertainties over the entire range.

Figure 5b shows the direct photon invariant yield from the internal conversion measurement [14] and compares it to theoretical calculations. With large significance, a direct photon spectrum is obtained for  $1 < p_T < 5 \text{ GeV}/c$ . The spectrum lies significantly above a  $T_{AA}$ -scaled NLO pQCD calculation [7] for  $p_T \lesssim 3 \text{ GeV}/c$ . The pQCD calculation indicates the contribution from hard scatterings. The lines show the scale uncertainty of the calculation. However, it is not clear how meaningful the comparison is down to this low  $p_T$  where the pQCD calculation reaches its limit of applicability. It is planned to replace the pQCD calculation by a reference measurement of direct photon production in  $p + p$  collisions with the same method as in Au + Au.

The excess of the measured direct photon spectrum above the pQCD calculation can be described by models that allow for a significant contribution of thermal photons. In order to describe thermal photon production in  $A + A$  collisions, the entire space-time evolution has to be accounted for including the hadronic phase. This is done in hydrodynamical models, which assume local thermal equilibrium. An important free parameter in such models is the initial temperature of the fireball. Figure 5b compares the measured direct photon spectrum to a 2 + 1 hydrodynamical model [15] for thermal-photon emission with an average initial temperature of  $T_0^{\text{ave}} = 360 \text{ MeV}$  ( $T_0^{\text{max}} = 570 \text{ MeV}$ ) and a formation time of  $\tau_0 = 0.15 \text{ fm}/c$ . The model underpredicts the data for  $p_T \gtrsim 3 \text{ GeV}/c$ . The data can be described when both sources, thermal and pQCD, are combined. Various other calculations come to similar descriptions with initial temperatures in the range  $370 < T_i < 570 \text{ MeV}$  [2, 16, 17]. The temperatures are significantly above the critical temperature for the QGP phase transition of  $T_c = 170 \text{ MeV}$ . However, the obtained temperature is only meaningful if the excess above pQCD is of thermal origin. Besides hard photons, also jet-plasma interactions may play a significant role [2].

## 4 Conclusions

The direct photon cross section in  $p + p$  collisions at  $\sqrt{s} = 200 \text{ GeV}$  is found to be consistent with a NLO pQCD cal-

<sup>3</sup> The preliminary result from the measurement of virtual photons is presented in the same figure in terms of  $\gamma_{\text{direct}}/\gamma_{\text{incl.}} + 1$ , which also indicates a direct photon excess as an enhancement above 1. Note that the two quantities are not exactly equivalent.

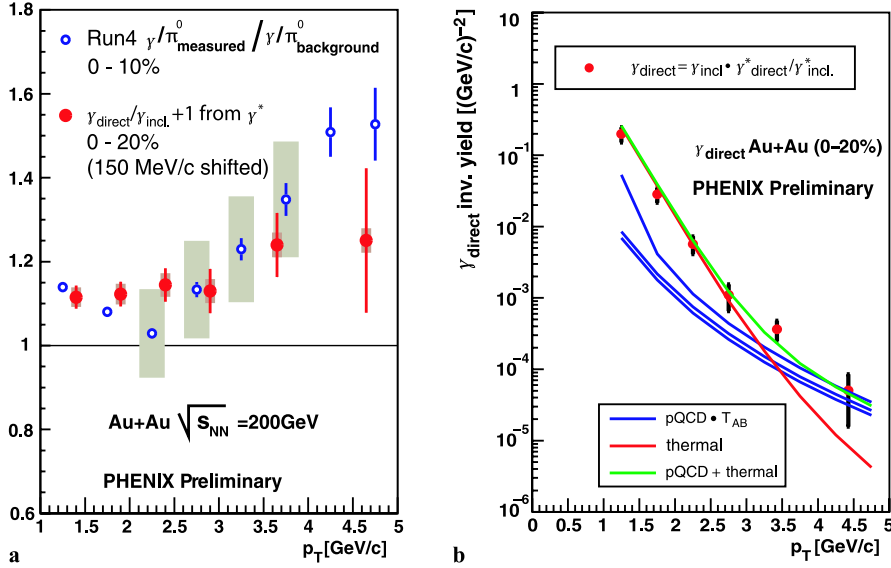


**Fig. 5.** **a** Direct photon excess for the conventional and the internal-conversion measurement in central Au+Au collisions [14]; **b** direct photon spectrum from the latter [14] compared to pQCD [7], thermal-photon [15], and the sum of both calculations

calculation over the entire range of the measurement from  $5 \text{ GeV} \leq p_T \leq 16 \text{ GeV}/c$ . In  $d + \text{Au}$  collisions, no indications for cold nuclear matter effects are found within the large uncertainties of the measurement. A high statistics  $d + \text{Au}$  run is planned. High  $p_T$  direct photon production in Au + Au collisions is found to scale with the nuclear overlap function  $T_{AA}$ , establishing medium effects as the cause for the hadron suppression observed in central Au + Au collisions.

At low  $p_T$  ( $1 \leq p_T \leq 5 \text{ GeV}/c$ ) a significant direct photon excess above the decay photon background is observed employing a new method in heavy ion collisions, which measures low invariant mass  $e^+e^-$  pairs from direct photon internal conversions. The signal appears to be above pQCD calculations for  $p_T \leq 3 \text{ GeV}/c$ , whose applicability is questionable, however, at this low  $p_T$ . If a thermal photon source modeled by hydrodynamical calculations is added to the pQCD calculation, the data can be described over the entire  $p_T$  range. Other direct photon sources like jet-plasma interactions might play a significant role as well.

## References

1. S. Turbide, R. Rapp, C. Gale, Phys. Rev. C **69**, 014903 (2004)
2. C. Gale, Nucl. Phys. A **774**, 335 (2006)
3. S.S. Adler et al., Phys. Rev. Lett. **91**, 072301 (2003)
4. S.S. Adler et al., Phys. Rev. Lett. **96**, 202301 (2006)
5. L. Aphecetche et al., Nucl. Instrum. Methods A **499**, 521 (2003)
6. K. Okada, hep-ex/0501066 (2005)
7. L.E. Gordon, W. Vogelsang, Phys. Rev. D **48**, 3136 (1993)
8. S.S. Adler et al., Phys. Rev. Lett. **94**, 232301 (2005)
9. J.H. Cobb et al., Phys. Lett. B **78**, 519 (1978)
10. C. Albajar, et al., Phys. Lett. B **209**, 397 (1988)
11. N.M. Kroll, W. Wada, Phys. Rev. **98**, 1355 (1955)
12. K. Adcox et al., Phys. Rev. C **69**, 024904 (2004)
13. S.S. Adler, et al., Phys. Rev. Lett. **94**, 082301 (2005)
14. S. Bathe, Nucl. Phys. A **774**, 731 (2006)
15. D. d'Enterria, D. Peressounko, nucl-th/0503054 (2005)
16. J. Alam, J.K. Nayak, P. Roy, A.K. Dutt-Mazumder, B. Sinha, nucl-th/0508043 (2005)
17. A.K. Chaudhuri, nucl-th/0512032 (2005)